# Q factor measurements, analog and digital<sup>1</sup>

## By Darko Kajfez

#### 1. Introduction

Resonators are the basic building blocks of rf filters and oscillators. Like any other circuit component, a resonator must be experimentally tested to determine its properties. The three fundamental characteristics of an rf resonator that have to be determined by measurement are: (1) resonant frequency, (2) coupling coefficient, and (3) unloaded Q factor.

Rf resonators used to be tested by specialized instruments, such as grid-dip meters and Q meters. Those devices have largely been replaced by more universal ones, network analyzers. At microwave frequencies, the Q factor used to be measured by precision slotted lines, but those, too, have been replaced by network analyzers.

Three possible circuit configurations are used for Q factor measurement: the transmission type, the reflection type, and the reaction type. As will be described in more detail later, for any of these configurations, a 3-point measurement can determine all the three needed numbers.

A novelty in Q-factor measurement is an overdetermined measurement procedure in which some 20 or more points are taken by an automatic network analyzer and then processed by a personal computer. The results of the data processing provide not only the three fundamental numbers, but also the estimates on their standard deviations and an estimate of the coupling losses.

## 2. Loaded, unloaded, and external Q

Lumped-element resonators consist of a combination of one capacitor and one inductor,

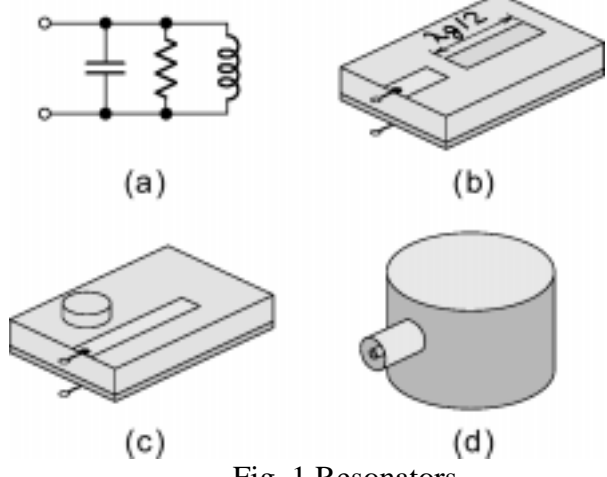


Fig. 1 Resonators

-

<sup>&</sup>lt;sup>1</sup> Copyright © Darko Kajfez 1999

such as in Fig. 1(a). A distributed-element resonator may be a simple half-wavelength microstrip transmission line, capacitively coupled to the input microstrip line, such as in Fig. 1(b). To achieve a higher Q factor, a dielectric resonator can be inductively coupled to the microstrip line, such as in Fig. 1(c). For high power handling, it may be necessary to employ a hollow cylindrical or rectangular cavity, such as in Fig. 1(d), in which the input is connected through a coaxial transmission line.

Figure 2(a) shows the equivalent circuit, which is appropriate for all the distributedelement resonators from Fig. 1. The figure also contains an external source consisting of  $V_s$  and internal impedance, which is matched to the input transmission line. This source would represent the network analyzer, which is connected to the input port 1 of the resonator. The transmission line of length l, located between input (port 1) and the location of the coupling (port 2) could be physically very short. This length is never known very precisely.

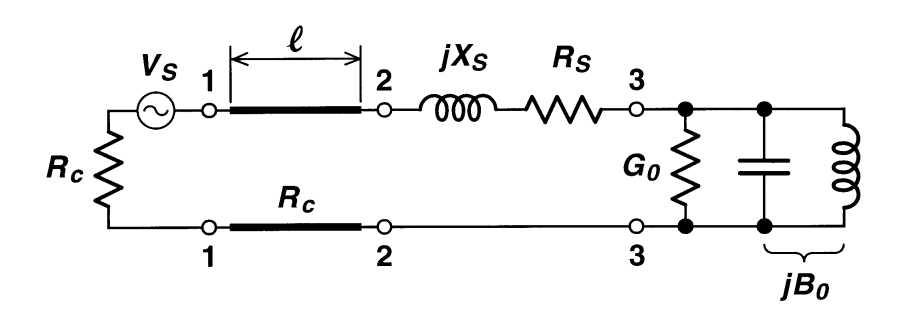


Fig. 2(a) A resonator and an external circuit

Port 3 is the location of the resonator itself. The impedance  $R_s+jX_s$  represents the transformation properties of the coupling mechanism. For a loop coupling,  $X_s$  is a positive reactance, and for a probe coupling,  $X_s$  is a negative reactance. The value of  $X_s$  can be considered to be constant in the frequency range of interest (say 1 % on each side of the resonant frequency). The reactance of the resonator, represented by a parallel LC combination, varies with frequency hundreds or even thousands time faster than  $X_s$ .

Suppose an observer can enter the resonator and look left and right from port 3. On the right hand side, he will see the unloaded resonator. Its resonant frequency is

$$f_0 = \frac{1}{2\pi\sqrt{LC}} \tag{1}$$

The unloaded Q factor is denoted  $Q_0$ :

$$Q_0 = \frac{2\pi f_0 C}{G_0} \tag{2}$$

The conductance  $G_0$  represents the dissipation inside the resonator proper. Typically, this dissipation is caused by conductor losses and by dielectric losses. The corresponding resistance is the inverse value,  $R_0 = 1/G_0$ .

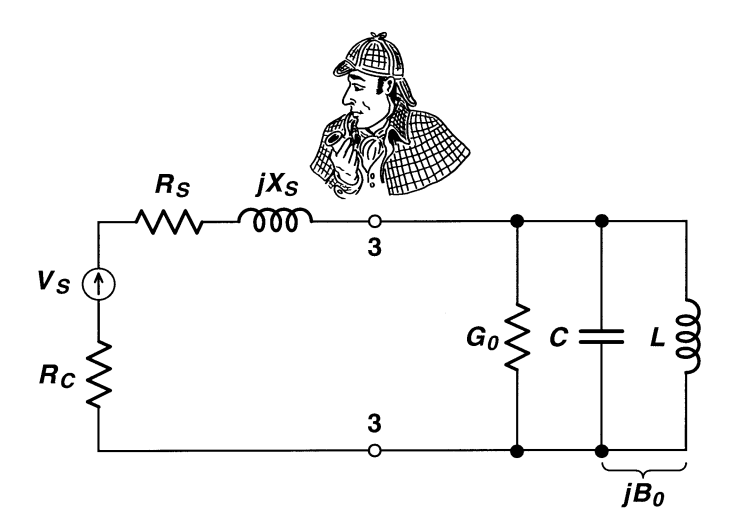


Fig. 2(b) Thevenin's equivalent circuit for port 3

If the observer at port 3 now turns to the left (toward port 1), he sees the series combination of resistance  $R_s$  and the reactance  $X_s$ , and behind them a transmission line terminated in a Thevenin source. As the source impedance is equal to the characteristic impedance of the transmission line, the length of the transmission line does not change the impedance seen by the observer: any length of a transmission line, which is terminated in a matched load, has the same input impedance, equal to  $R_c$ .

Using elementary circuit theory operations, the external circuit that the observer saw, can be now replaced by a Norton's equivalent, consisting of a current source in parallel with the impedance, as shown in Fig. 2(c). As a further simplification, the impedance  $R_c+R_s+jX_s$  can be transformed into admittance  $G_{ex}+jB_{ex}$  shown in Fig. 2(c), the external admittance felt by the resonator.

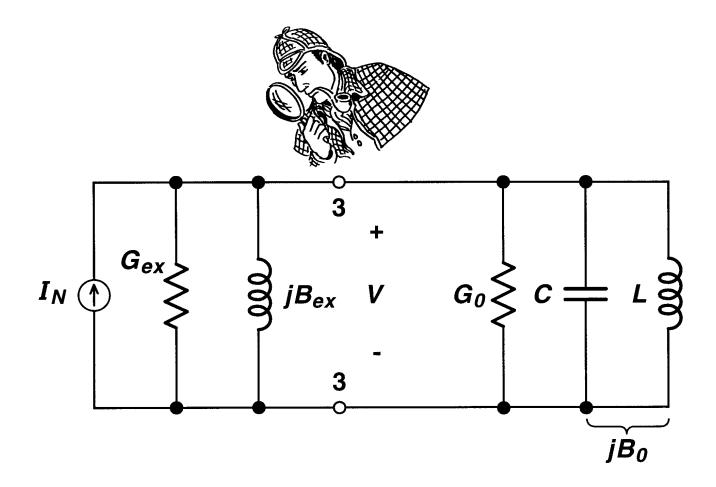


Fig. 2(c) Norton's equivalent circuit for port 3

Now, the observer at port 3 can clearly see that the external circuit influences the resonator in two ways. First, the susceptance  $B_{ex}$  detunes the resonant frequency. However, this frequency shift is so small, that it is of little consequence. The observer simply has to deal with a new, loaded resonator that has slightly different resonant frequency. Second, conductance  $G_{ex}$  comes in parallel to  $G_0$ , thus lowering the overall Q to a new value  $Q_L$ , which is expressed by writing

$$\frac{1}{Q_L} = \frac{1}{Q_0} + \frac{1}{Q_{ex}} \tag{3}$$

The external Q factor is defined in analogy with (2):

$$Q_{ex} = \frac{2\pi f_0 C}{G_{ex}} \tag{4}$$

The ratio of power dissipated in the external circuit to the power dissipated in the resonator is called coupling coefficient  $\kappa$ . As both  $G_0$  and  $G_{ex}$  have common voltage V, the ratio of powers is proportional to the ratio of conductances:

$$\kappa = \frac{V^2 G_{ex}}{V^2 G_0} = \frac{G_{ex}}{G_0} = \frac{Q_0}{Q_{ex}}$$
 (5)

When an equal amount of power is dissipated in the external circuit as in the resonator itself, the coupling is said to be critical, and the coupling coefficient in this case is  $\kappa=1$ . An undercritical coupling means that more power is dissipated in the resonator than in the external circuit, while an overcritical coupling means that more power is lost in the external circuit than in the resonator.

By eliminating  $Q_{ex}$  from (3) with the use of (5), one obtains the relationship between the unloaded and the loaded Q as follows:

$$Q_0 = Q_L \left( 1 + \kappa \right) \tag{6}$$

As soon as one starts a measurement, the resonator is loaded by the external circuit (here the network analyzer), and the measurement will produce the loaded Q,  $Q_L$ . The stronger the coupling one creates between the network analyzer and the resonator, the lower the value of the measured loaded Q. To find the unloaded Q, the measurement should be designed in such a way, that it also provides the value of the coupling coefficient  $\kappa$ . Then, using  $Q_L$  and  $\kappa$ , one computes  $Q_0$  from (6). This is how most Q factor measurements are done [1-3].

### 3. Transmission-type measurement

Suppose a manufacturer of the microstrip substrate wants to measure the Q factor of a transmission line fabricated from his material. He would probably create a half-wavelength resonator two-port, something like the one shown in Fig. 3(a). Port A is the input, and port B is the output. The network analyzer is connected at both sides, and the transmission coefficient  $S_{2I}$  is measured. The equivalent circuit of such a measurement is shown in Fig 3(b). For the sake of simplicity, the coupling-loss resistors on the input and output sides have been ignored.

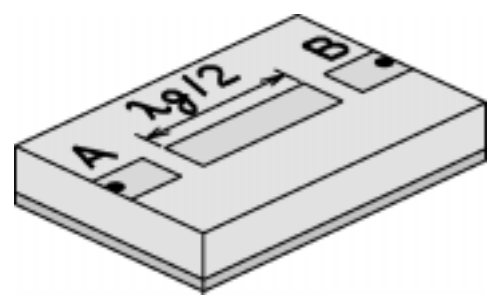


Fig. 3(a) Microstrip half-wavelength two-port resonator

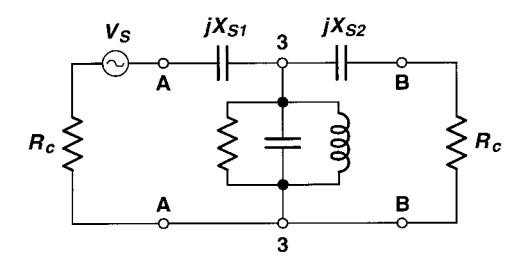


Fig. 3(b) Thevenin's equivalent for half-wavelength resonator

As before, one can change Thevenin equivalent into Norton equivalent, and obtain Fig. 3(c).

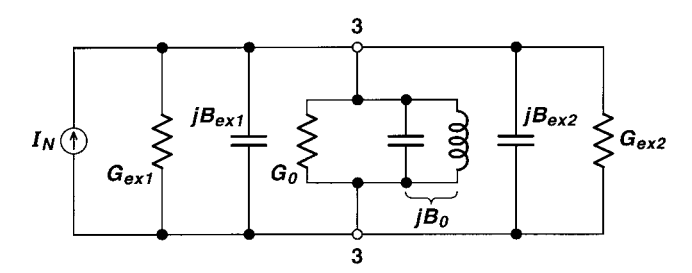


Fig. 3(c) Norton's equivalent for half-wavelength resonator

Suppose the observer at port 3 (the resonator port) wears very special tinted glasses, tuned to the resonant frequency of the loaded resonator. He will not see any susceptances, because they cancel each other at that frequency. All that he will see are the three conductances shown in Fig. 3(d). Since they are connected in parallel, the corresponding powers are proportional to the conductance values, and one can therefore define the input and output coefficients as follows:

$$\kappa_{1} = \frac{G_{ex1}}{G_{0}} = \frac{Q_{0}}{Q_{ex1}} \tag{7}$$

$$\kappa_{1} = \frac{G_{ex1}}{G_{0}} = \frac{Q_{0}}{Q_{ex1}}$$

$$\kappa_{2} = \frac{G_{ex2}}{G_{0}} = \frac{Q_{0}}{Q_{ex2}}$$
(8)

The overall coupling coefficient, to be used in (6), is the sum of the two:

$$\kappa = \kappa_1 + \kappa_2 \tag{9}$$

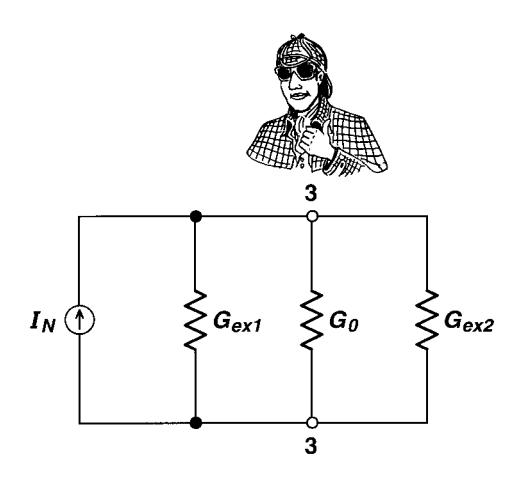


Fig. 3(d) Equivalent circuit for port 3 at resonance

The magnitude of the forward transmission gain  $S_{21}$  displays a familiar resonance effect as a function of frequency, indicated in Fig. 4. The loaded Q of the system is inversely proportional to the difference between the 3-dB frequencies  $f_1$  and  $f_2$  at each side of the resonance:

$$Q_L = \frac{f_0}{f_2 - f_1} \tag{10}$$

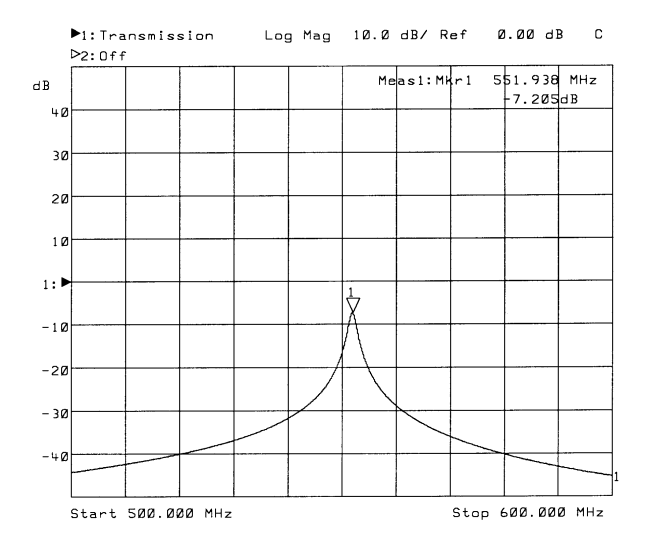


Fig. 4 Transmission-type measurement,  $S_{21}$  amplitude plot

Now that  $Q_L$  has been determined, one needs to find  $\kappa$ . That can be computed from the magnitude  $S_{2I}$  at the center frequency. It follows from Fig. 3(d) that the magnitude of  $S_{2I}$  at the resonant frequency is

$$S_{21}(f_0) = \frac{2\sqrt{\kappa_1 \kappa_2}}{1 + \kappa_1 + \kappa_2} \tag{11}$$

Through a careful fabrication procedure, one can make the input and output air gaps equal to each other, so that

$$\kappa_1 = \kappa_2 \tag{12}$$

For such a symmetrical coupling, one obtains

$$\kappa = 2\kappa_1 = \frac{S_{21}(f_0)}{1 - S_{21}(f_0)} \tag{13}$$

and when this is substituted into (6), the unloaded Q can be computed as follows:

$$Q_0 = \frac{Q_L}{1 - S_{21}(f_0)} \tag{14}$$

This is the unloaded Q of the microstrip resonator, the number that the manufacturer of the substrate wanted to know.

Usually, the magnitude of  $S_{2I}(f_0)$  is expressed in decibels and called insertion loss  $\alpha$ . Since  $S_{2I}$  is always smaller than unity,  $\alpha$  is a negative number. Then, to compute  $S_{2I}(f_0)$  one uses the following expression:

$$S_{21}(f_0) = 10^{\frac{\alpha}{20}} \tag{15}$$

For the transmission-type measurement to be accurate, condition (12) must be satisfied, requiring that the input and output couplings equal each other. In this measurement, there is no electrical verification of this equality; one must trust that the mechanical tolerances are tight enough to insure the equality. Another important factor to keep in mind is that the accuracy is seriously reduced when coupling is larger than critical. This happens because  $S_{21}(f_0)$  approaches unity as the coupling becomes strong. Therefore, the denominator of (14) becomes a difference of two almost equal numbers, so that even a small error in  $S_{21}(f_0)$  will cause a large error in  $Q_0$  (even though  $Q_L$  has been measured accurately).

## 4. Reflection-type measurement

For this measurement the resonator only needs one port. When the network analyzer is attached to this port, the equivalent circuit looks the same as shown in Fig. 2(a). The measurement procedure is well documented in microwave measurement handbooks such as Ginzton [1], Sucher and Fox [2], or Matthaei, Young and Jones [3]. Although these books were written before the first network analyzer was made, the principles involved remain unchanged from the slotted-line and admittance-bridge era. With few modifications, the reflection-type measurement can be performed with a network analyzer [4]. The beauty of this measurement is a perfect circle that the measured reflection coefficient, plotted on a Smith chart, describes as a function of frequency. If you don't see a perfect circle, there is something wrong with your calibration or your reference position!

Figure 5 shows a measured input reflection coefficient  $S_{II}$  (a complex number) as seen on the polar display of a network analyzer. The center of the Q circle is rotated by an angle  $\theta$  with respect to the real axis of the Smith chart. Two circuit elements from Fig. 2(a) may cause this rotation. First, the length of the transmission line l between the coupling loop and the reference position (input coaxial connector) rotates  $S_{II}$  by an angle  $-2\beta l$ , where the symbol  $\beta$  denotes the propagation constant of the line. Second, the reactance  $X_s$  rotates and also shrinks the circle. Anyway, the rotation is of no importance for the determination of  $Q_L$  and  $\kappa$ . To determine the value of  $Q_L$  it is necessary to identify three points on the Q circle. As shown in Fig. 5, the first of those points is center frequency  $f_0$ =460.65 MHz, the one identified by Marker 1. The other two frequencies,  $f_I$  and  $f_2$ , belong to the two points inclined by  $\phi$ =45 degrees on each side of the centerline. Then, the loaded Q is computed by (10).

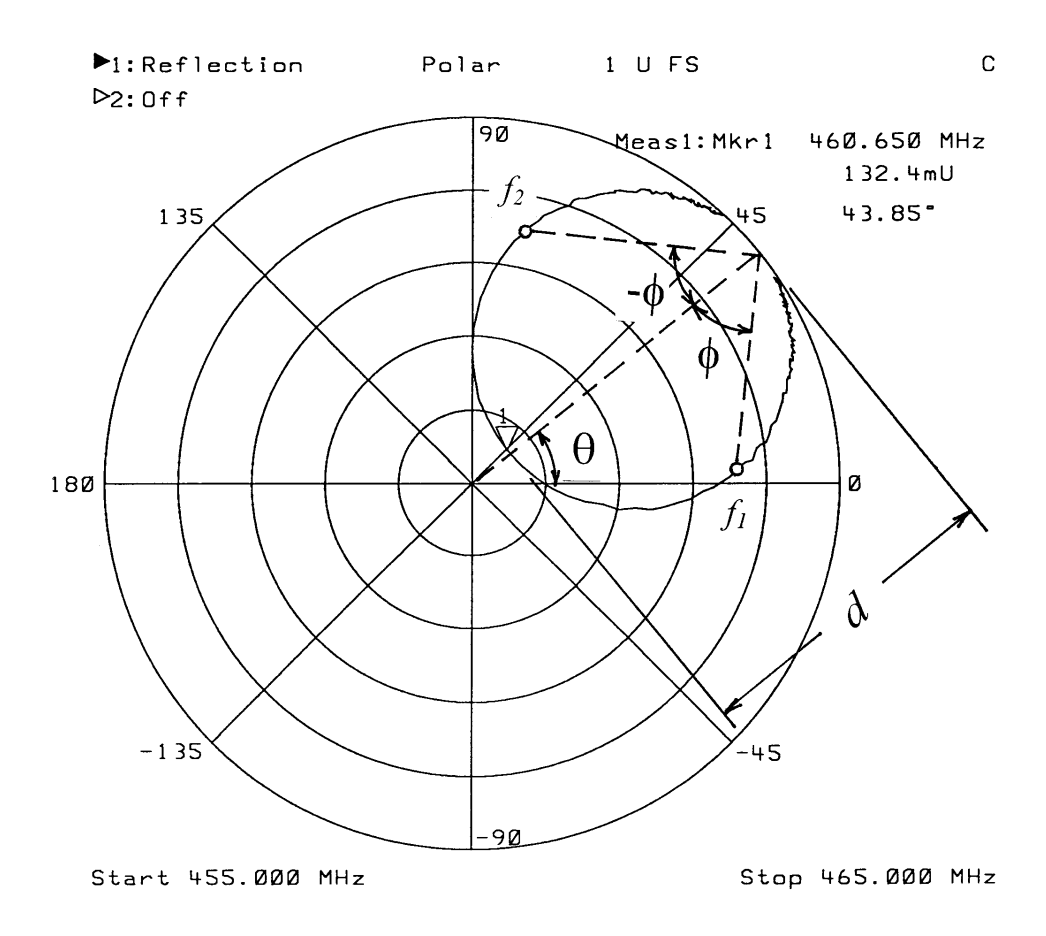


Fig. 5 Reflection-type measurement,  $S_{II}$  polar plot

To find the coupling coefficient, one has to measure the diameter d of the Q circle. Weakly coupled resonators will produce small Q circles, and strongly coupled resonators large ones. The equation for computing the coupling coefficient  $\kappa$  from the measured value of d can be found in reference [4]:

$$\kappa = \frac{1}{\frac{2}{d} - 1} \tag{16}$$

The unit of length in this case is the radius of the Smith chart. Thus, when d=1, the point  $f_0$  is located at the center of the Smith chart and the coupling coefficient is  $\kappa=1$  (critical coupling).

Thus, Ginzton's reflection-type measurement of Q is also a three-point method. In its original version, the Q circle was drawn by hand on the Smith chart point by point. The points were identified by their corresponding frequencies. To find the frequencies of the  $\phi$ =±45° it was necessary to graphically construct a linear scale for frequencies perpendicular to the  $\phi$ =0 line, and then interpolate between the nearest measured points. On the polar display of a network analyzer, the angle  $\phi$  is not available, since the display gives only information on the inclination angle  $\theta$  of reflection coefficient  $S_{11}$ , measured from the center of the Smith chart. A useful program has been developed by Asija and Gundavajhala [5], which can be used to simplify reading data from a network analyzer and to perform the subsequent computation of  $Q_L$  and  $Q_0$ .

## 5. Reaction-type measurement

When a dielectric resonator is mounted close to a microstrip transmission line such as in Fig. 6, it is possible to measure the Q factor directly, by connecting the network analyzer on both ends of the microstrip. The configuration shown in Fig. 6 was proposed by Podcameni et al. [6], and analyzed in more detail by Khanna and Garault [7].

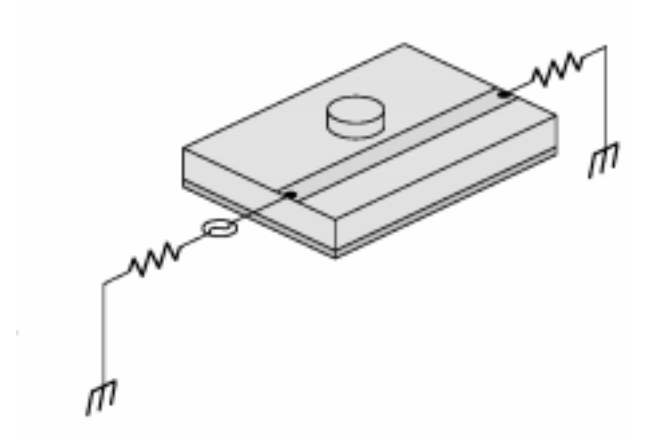
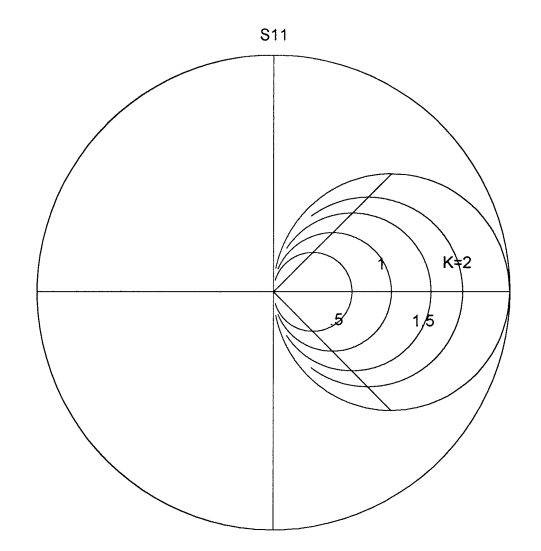


Fig. 6 Reaction-type measurement

The measured value of  $S_{II}$ , shown on the polar display of the network analyzer, also displays Q circles, and the stronger the coupling, the larger the diameter of the Q circle. Figure 7(a) shows several circles for couplings  $\kappa$  between 0.5 and 2. Also, the figure shows  $\phi=\pm 45^{\circ}$  lines to read the frequencies  $f_I$  and  $f_2$  for the determination of  $Q_L$ . Likewise, if the transmission coefficient  $S_{2I}$  is observed on the polar display shown in Fig. 7(b), the Q circles are clearly visible, but bunched toward the right-hand side. In both figures, all the circles are about half the size of those in the reflection-type

measurement. For instance, the largest theoretically possible diameter of the Q circle for the reaction-type measurement is d=1 (for an infinitely strong coupling), and for the critical coupling, the diameter is d=0.5. Although the resolution of the measurement may be reduced because of the smaller circles, this is nevertheless a convenient procedure. The resonator is mounted in exactly the same environment as will be used in a typical oscillator or filter design.



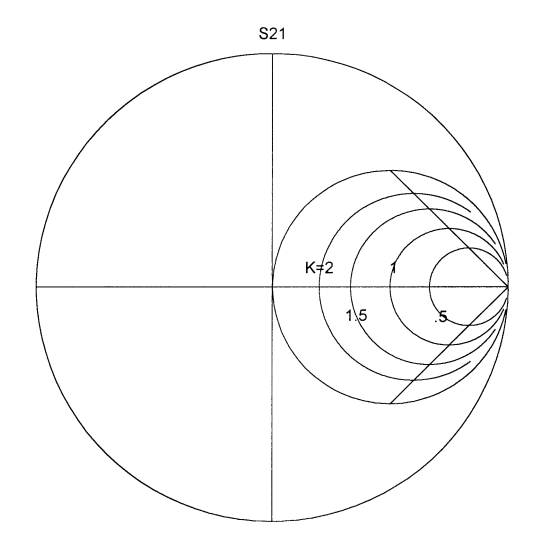


Fig 7(a) Reaction-type measurement, plot of  $S_{II}$ 

Fig. 7(b) Reaction-type measurement, plot of  $S_{21}$ 

Another advantage of this type of measurement is that the  $\phi=\pm 45^{\circ}$  angles coincide with the  $\theta=\pm 45^{\circ}$  angles of the input reflection coefficient  $S_{II}$ . Therefore, the frequencies  $f_I$  and  $f_2$  can be read directly from the network analyzer display, without the need for an additional program to change from  $\theta$  to  $\phi$  as in [5].

Reference [6] also describes a procedure for scalar reaction-type measurements, using only the amplitudes of  $S_{11}$  and  $S_{21}$  for determining the loaded and unloaded Q.

## **6.** The role of $X_s$

According to elementary circuit theory, the value of external susceptance  $G_{ex}$ , loading the resonator in Fig. 2(c), is given by

$$G_{ex} = \frac{R_c + R_s}{\left(R_c + R_s\right)^2 + X_s^2}$$
 (17)

Therefore, the coupling coefficient, as defined by (5), becomes

$$\kappa = \frac{G_{ex}}{G_0} = \frac{R_0}{R_c} \cdot \frac{1 + \frac{R_s}{R_c}}{\left(1 + \frac{R_s}{R_c}\right)^2 + \left(\frac{X_s}{R_c}\right)^2}$$
(18)

If  $(X_s/R_c)$  and  $(R_s/R_c)$  are negligibly small quantities, then the coupling coefficient is simply

$$\beta = \frac{R_0}{R_c} \tag{19}$$

The symbol  $\beta$  has traditionally been used to denote the coupling coefficient when the equivalent circuit does not contain the series reactance  $X_s$ . For the full equivalent circuit, which also takes into account that reactance, it is safer to use a new symbol,  $\kappa$ , based on the definition of coupling coefficient derived from a ratio of powers, as in (5). Furthermore, symbol  $\beta$  is easy to confuse with the propagation constant of the input transmission line.

To demonstrate the influence of  $X_s$  on the Q-circle size and position, the reflection coefficient as "seen" by the network analyzer at port 1 in Fig. 2(a) has been computed for several values of  $X_s$ . For simplicity, the coupling losses were ignored ( $R_s$ =0) and the length of the transmission line was set to zero. The characteristic impedance of the line was set to  $R_c$ =1 and the resonator losses were represented by  $R_0$ =1.5. Four different values of  $X_s$  were shown:  $X_s$ =0, 0.5, 1, and 2. The resulting Q circles are shown in Fig. 8.

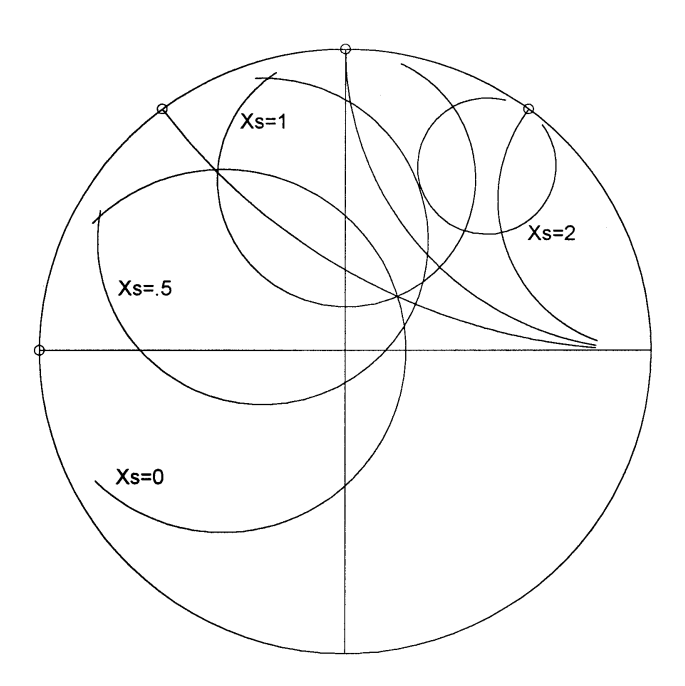


Fig. 8 Reflection-type measurement, influence of  $X_s$ 

For the vanishing reactance,  $\kappa = \beta = 1.5$  so that both definitions of the coupling coefficient give the same result. The Q circle is centered on the real axis, and its diameter is d=1.2. The difference between the two definitions becomes noticeable for  $X_s=0.5$ , because the Q circle is rotated, and its diameter is now only d=1.09. For a large reactance, such as  $X_s=2$ , the diameter shrinks further to d=0.667, and the corresponding coupling coefficient is

only  $\kappa=0.5$ . If the inadequate definition (19) were used, the coupling coefficient for all four cases would be equal to  $\beta=1.2$ .

One has to keep in mind that port 1 is the only terminal that can be either measured, or incorporated into an external circuit, such as an oscillator or a filter. Port 3 is simply not amenable to any measurement. There is no such thing as an observer who can sneak into the resonator, sit on port 3 and tell us how big  $X_s$  is. A practical answer to this dilemma is to accept the coupling coefficient such as predicted by the size d of the measured Q circle. To avoid the apparently impossible task of finding the accurate value of  $X_s$ , one should allow the length of the transmission line to be increased by the amount needed to rotate the observed Q circle back to the real axis. At this new reference position (which used to be called "the detuned short position"), one may use the equivalent circuit without  $X_s$ . At the same time, one should be aware that the loaded resonant frequency  $f_L$  is theoretically different from the unloaded resonant frequency  $f_0$ . This difference can be ignored for all practical purposes, at least within the first three digits of  $f_0$ .

The role of the coupling resistance  $R_s$  has a different effect. Namely,  $R_s$  detaches the Q circle from the outside rim of the Smith chart. This fact is used in the overdetermined measurement procedure to estimate the severity of coupling losses, as will be described in what follows.

# 7. Overdetermined procedures

Common to all the measurement procedures described until now is the fact that one has to measure manually some S parameter at frequencies  $f_0$ ,  $f_1$  and  $f_2$  and then compute the values of  $Q_L$  and  $\kappa$ . These procedures may commonly be called "three-point procedures." They were all developed during the era of analog instrumentation.

Today's network analyzers are all computer controlled and therefore digital instruments. They can measure almost instantly up to 1600 frequency points and either store them, or deliver them to a file to be read by another computer. Data processing can then be used to determine the center and the diameter of the circle on the Smith chart, interpolate the exact position of frequency points  $f_0$ ,  $f_1$ , and  $f_2$ , and utilize any appropriate equation for an accurate computation of  $Q_L$  and  $\kappa$ . Because more than three points are needed in such an operation, these procedures may be called "overdetermined." Typically, 20 or more points are used, but any number larger than three should work. Early attempts of overdetermined Q-factor measurements can be found in [8-10]. General-purpose, commercially available programs QZERO and SCALARQ are distributed with the book Q Factor [11]. Both programs are intended for processing of reflection-type measurements.

The input data for the QZERO program should be arranged in a file that contains three columns of numbers (in ASCII format) as follows:

```
f \operatorname{Real}(S_{11}) \operatorname{Imag}(S_{11})
```

Any network analyzer automatically chooses an equidistant set of frequencies, but QZERO can also operate when the frequencies are not equally spaced. For instance, if one or several of the data look suspicious, that particular data line, or even a block of data lines, can be erased from the file without any detrimental effect on QZERO.

The program first finds an estimate of the loaded resonant frequency  $f_L$ , and then computes three complex coefficients  $a_1$ ,  $a_2$ , and  $a_3$  in the following equation:

$$S_{11}(t) = \frac{a_1 t + a_2}{a_3 t + 1} \tag{20}$$

Variable t is the relative frequency detuning with respect to the loaded resonant frequency  $f_L$  defined as follows:

$$t = 2\frac{f - f_L}{f_L} \tag{21}$$

The procedure is iterated several times: each time a new value of the weighting factor is computed to emphasize the points close to the resonance, and to suppress the influence of points far from the resonance. The resulting values of  $Q_L$ ,  $Q_0$ ,  $\kappa$ , and  $f_L$  are displayed on the left-hand side of the Smith chart, as seen in Fig. 9. In that figure, one can see the input data (indicated by black dots), and the best-fit circle (plotted by a solid line).

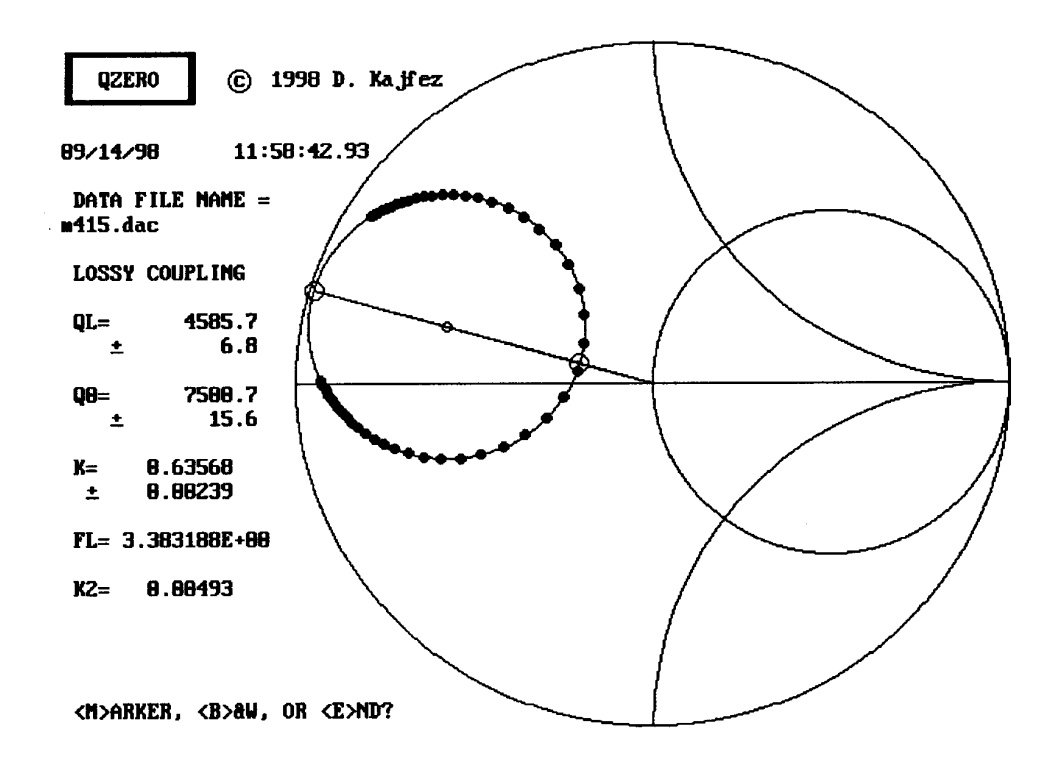


Fig. 9 Overdetermined measurement, display of QZERO program

Two characteristic points on the Q circle, namely the  $f_L$  and the "detuned short" are indicated by larger dots, and the center of the Q circle is indicated by a smaller dot. A quick glance at the Smith chart is sufficient to check whether the data fit is satisfactory, or whether something is wrong.

A side benefit of an overdetermined procedure is the possibility to statistically estimate the standard deviations for all the quantities of interest. For instance, the value of  $Q_L$  in Fig. 9 is estimated to be 4585.7  $\pm$  6.8, while  $Q_0$  is 7500.7  $\pm$  15.6. It should be emphasized that these uncertainties describe only the random errors and not the systematic errors. The systematic errors of various models of network analyzers differ from each other, and they also depend on the frequency of operation. A separate analysis of systematic errors would be required in order to see what effect they have on the resonator characteristics. Program QZERO does not have the provision for such an analysis of systematic errors.

As mentioned in the previous section, the coupling losses (modeled by the presence of resistor  $R_s$ ) can cause the Q circle to be detached from the perimeter of the Smith chart. Figure 10 shows the effect of coupling losses when  $R_s$ =0.04,  $X_s$ =0.8,  $R_o$ =0.75 and  $R_c$ =1.

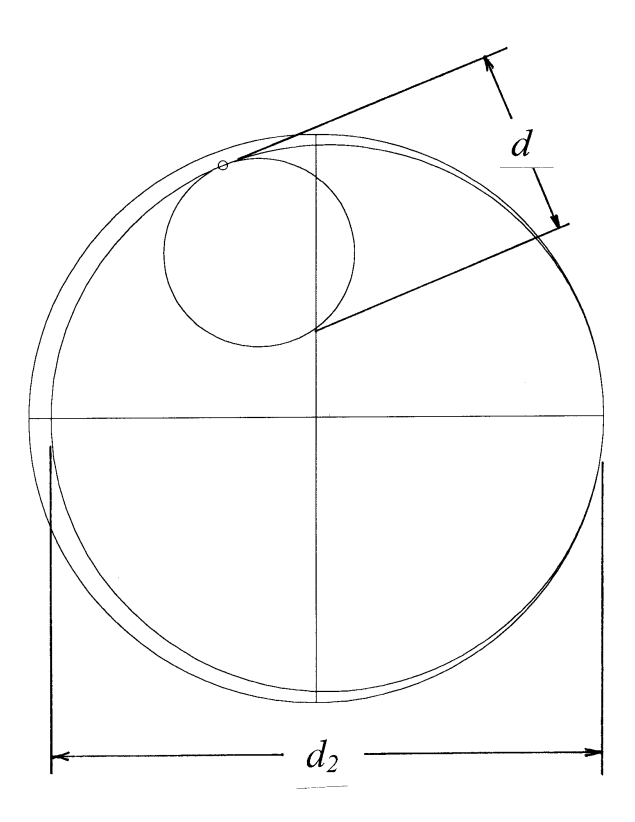


Fig. 10 Reflection-type measurement, effect of lossy coupling

Once the center and diameter d of the Q circle are known, it is possible to evaluate diameter  $d_2$  of an auxiliary circle which is tangential both to the Q circle and to the Smith

chart perimeter. The diameter  $d_2$  is now used to find the overall coupling coefficient  $\kappa$  [11]:

$$\kappa = \frac{1}{\frac{d_2}{d} - 1} \tag{22}$$

For the special case when coupling losses are negligible, the auxiliary circle coincides with the perimeter of the Smith chart, so that  $d_2=2$ , and (22) becomes identical with (16).

For carefully manufactured resonators, the coupling losses should be small, of the order of  $R_s/R_0 < 0.01$ . The overall coupling coefficient of a reflection type resonator now consists of two parts:

$$K = K_1 + K_2 \tag{23}$$

where  $\kappa_1$  is the coupling that describes the power loss in the external circuit, and  $\kappa_2$  describes the power loss in the coupling mechanism (this can be a loop, probe, gap capacitance, waveguide iris or similar). The ratio of  $\kappa_2$  to  $\kappa_1$  is proportional to the ratio of resistances  $R_s$  and  $R_c$ :

$$\frac{\kappa_2}{\kappa_1} = \frac{R_s}{R_c} \tag{24}$$

The value of  $\kappa_2$ =0.00493 is also shown on the display of QZERO in Fig. 9. This number is clearly an approximation, and the program does not attempt to find its standard deviation. Nevertheless, the value may be of use to a design engineer who wants to compare several different versions of coupling to the same resonator. In the example shown, approximately 0.5 percent of the total power is dissipated in the resistance of the coupling loop.

The program SCALARQ is intended for processing data taken with a scalar network analyzer, that measures only the amplitude (but not the phase) of the reflection coefficient  $S_{II}$ . The theory of operation can be found in [12]. An example of the display obtained by SCALARQ can be seen in Fig. 11. This example utilizes the same input data as in Fig. 9, except that the phase information is ignored. The measured data points are again shown by black dots, and a solid line shows the best-fit curve. Since the phase of the reflection coefficient is not known, one cannot plot the results on a Smith chart. Thus, one cannot tell whether this reflection coefficient represents an overcoupled or an undercoupled case. There are two possible interpretations of the measured data, and the display of SCALARQ shows both of them. Another, independent, experiment must be performed in order to decide which of the two answers is correct. Except for this limitation, the accuracy of the results obtained by SCALARQ is of the same order as the one obtained by QZERO. The resulting  $Q_0$ =7500.9 for the undercoupled case agrees very well with the value  $Q_0$ =7500.7 obtained in Fig. 9.

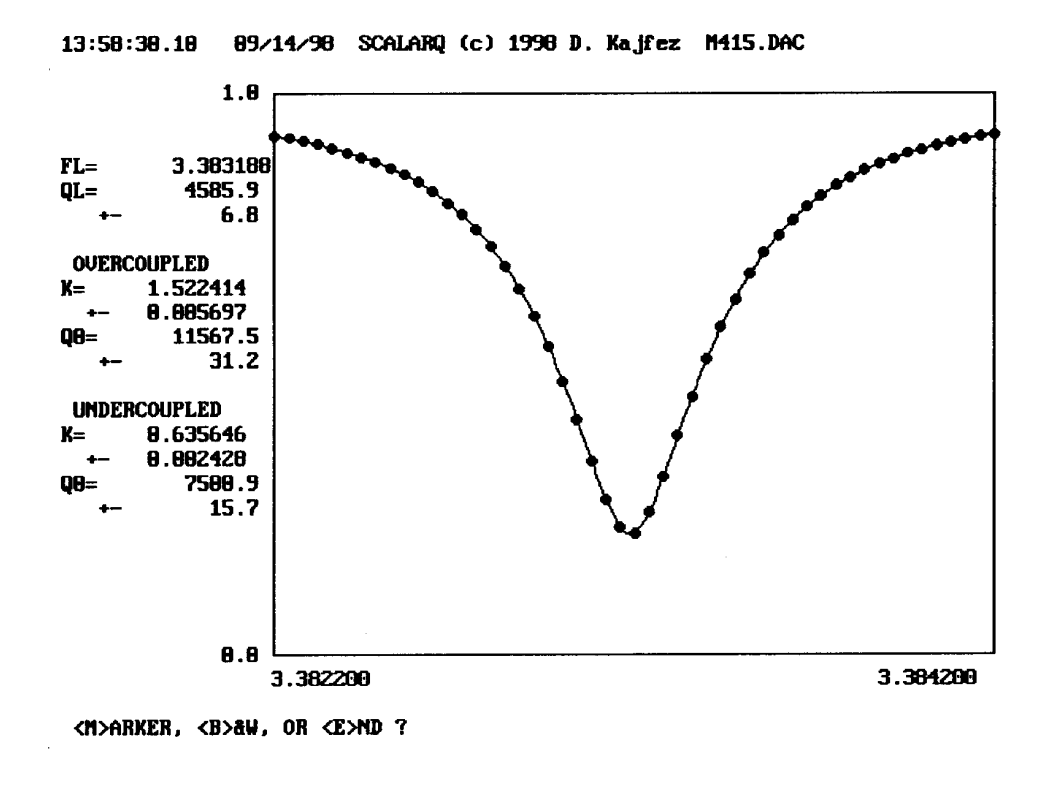


Fig. 11 Overdetermined measurement, display of SCALARQ program

Finally, it is good to keep in mind another advantage of the overdetermined procedures, namely their robustness to noisy data. In Fig. 12 a random noise of 0.04 has been artificially added to each of the input data from Fig. 9. In spite of the added noise, the results computed by QZERO are still very close to those obtained without noise. On the other hand, the estimated uncertainties are all larger than before, as expected.

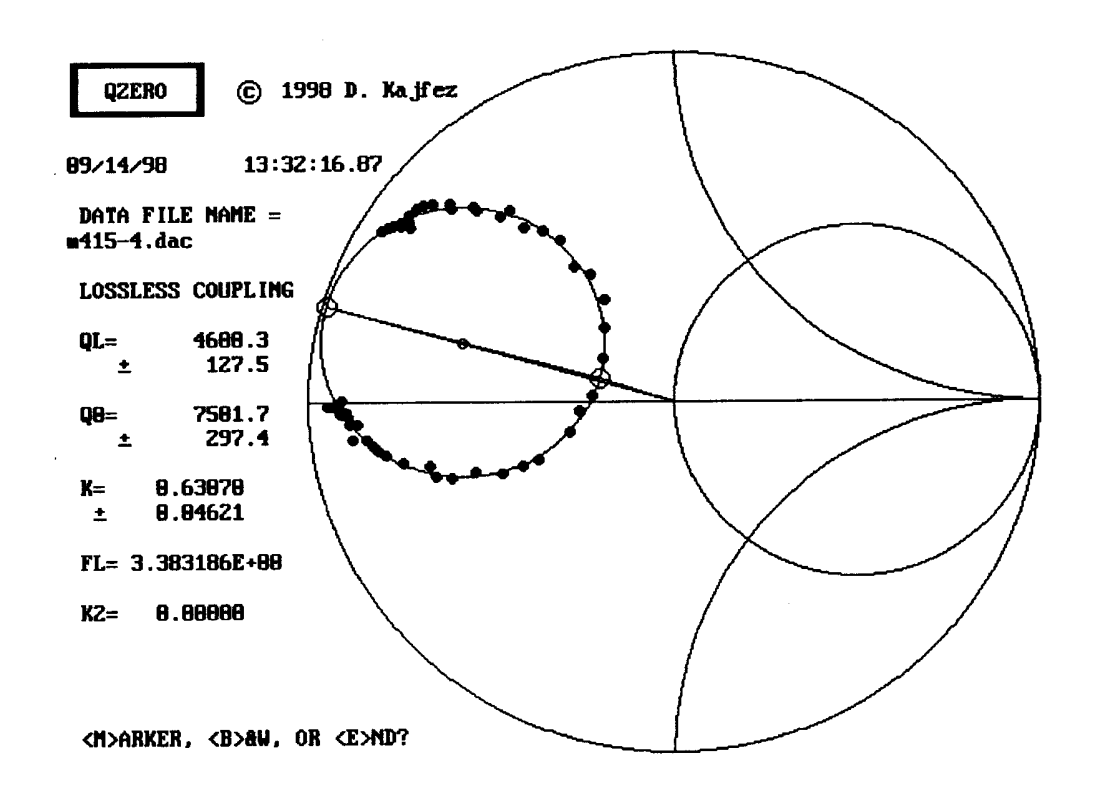


Fig. 12 Reflection-type measurement, effect of noisy data

### **References:**

- [1] E. L. Ginzton, *Microwave Measurements*. New York: McGraw-Hill, 1957. See Chapter 9.
- [2] M. Sucher, and J. Fox (eds.), *Handbook of Microwave Measurements*. New York: Polytechnic Press, 1963. See Chapter 7.
- [3] G. L. Matthaei, L. Young and E. M. T. Jones, *Microwave Filters, Impedance-Matching Networks, And Coupling Structures*. New York: McGraw-Hill, 1964. See Chapter 11.
- [4] D. Kajfez and E. J. Hwan, "Q-factor measurement with network analyzer," *IEEE Trans. Microwave Theory Tech.*, vol. MTT-32, pp. 666-670, July 1984.
- [5] A. Asija and A. Gundavajhala, "Quick measurement of unloaded Q using a network analyzer," *Rf Design*, pp. 48-52, October 1994.
- [6] A. Podcameni, L. F. M. Conrado, and M. M. Russo, "Unloaded quality factor measurement for MIC dielectric resonator application," *Electronics Letters*, vol. 17, pp. 656-658, 1981.
- [7] A. P. S. Khanna and Y. Garault, "Determination of loaded, unloaded and external quality factors of a dielectric resonator coupled to a microstrip line," *IEEE Trans. Microwave Theory Tech.*, vol. MTT 31, pp. 261-264, March 1983.

- [8] W. P. Wheless and D. Kajfez, "Microwave resonator circuit model from measured data fitting," *1986 IEEE MTT-S Symposium Digest*, pp. 681-684, Baltimore, June 1986.
- [9] M. C. Sanchez, E. Martin, and J. Zamarro, "New vectorial automatic technique for characterisation of resonators," *IEE Proc. H.*, vol. 136, pp. 145-150, April 1989.
- [10] C. P. Hearn, P. G. Bartley, and E. S. Bradshaw, "A modified Q-circle measurement procedure for greater accuracy," *Microwave Journal*, vol. 36, pp. 108-113, October 1993.
- [11] D. Kajfez, *Q Factor*, Oxford, MS: Vector Forum, 1994.
- [12] D. Kajfez, "Q factor measurement with a scalar network analyser," *IEE Proc.-Microw. Antennas Propag.*, vol. 142, pp. 369-372, October 1995.

# About the author

Darko Kajfez is emeritus professor of electrical engineering at the University of Mississippi. He can be reached by e-mail at *eedarko@olemiss.edu*. His mailing address is:

Dr. Darko Kajfez P. O. Box 757 University, MS 38677 USA.